Radiation Sensors Based on GaN Microwires

Extended abstract

Dirkjan Verheij[1]
[1] *Instituto Superior Técnico, Campus Tecnológico e Nuclear, Bobadela LRS, Portugal*
(Dated: November 2017)

GaN microwires, grown by Metal Organic Chemical Vapour Deposition (MOCVD) and with diameters between 1 and 2 μm, were used to fabricate radiation sensor by electrically connecting their extremities using photolithography. The most important parameters to analyse are the gain, the response time and decay time of the sensors. As GaN has a bandgap of 3.4 eV a very low gain for radiation with $\lambda > 365$ nm is expected and a high gain for more energetic radiation. The photocurrent behaviour of single wire sensors were studied under visible and UV illumination and under irradiation with protons. The fabricated devices demonstrated proper UV detection and decay times below 10 seconds were measured. However underwhelming photocurrent gain factors (<20%) were achieved. The irradiation with protons caused a significant degradation of the devices but the results confirmed their potential as particle detector, as similar decay times and higher gain factors were achieved in comparison with the UV detection. Photoconductivity measurements after the irradiation resulted in an overall improvement of the devices regarding their response to UV radiation. The photocurrent gain factors increased to approximately twice the value that was obtained prior to the irradiation and some quenching of the persistent photocurrent was observed. The results indicate the possibility of using GaN microwires not only as UV detectors, but also as a particle detectors.

I. INTRODUCTION

The continuous downscaling in size of what we can build and produce with micro- and nanotechnology has fomented an incredibly big amount of research that tries to connect things we barely see with microscopes to real life applications. Part of this research is dedicated to Gallium nitride (GaN) structures. GaN is a wide direct bandgap semiconductor and has been applied in high efficiency ultraviolet (UV) light-emitting and sensing applications since the nineties[1, 2]. However, over the last decade, its nano- and microwire configuration have attracted intense attention. Nano- and microwires are unique structures due to their large surface-to-volume ratio and high crystalline quality. Furthermore, they are excellent building blocks for bottom-up fabrication approaches[3]. These properties, together with high stability and radiation resistance, make GaN wires very interesting for application in UV photodetectors and radiation sensors[4].

In comparison to their bulk counterparts, GaN nanowire-based photodetectors have achieved higher photoconductive gain[4]. Nonetheless, these devices also present several limitations such as large decay times and the existence of a persistent photocurrent, *i.e.*, an increased current level that persists even when the external stimulus is switched off [5]. Furthermore, when assembling a device, special care must be taken when depositing the contacts as typically it will modify surface state properties, which can harm the reproducibility characteristics of the radiation sensor[6]. In addition, two very important parameters to create commercially interesting sensors are gain and response time. In general, in nanowire sensors there has been a fundamental trade-off between the photoconductive gain and speed of photodetectors, as the increase of one of those parameters usually decreases the other[7].

So far, the potential of GaN nanowire-based photodetectors has already been demonstrated, however, very little investigation has been done on the sensing capabilities of GaN nanowires to heavy particles such as protons, neutrons and ions. Consequently, the assembly of a radiation sensor which can detect heavy particles can potentially fill in this gap. If the detection of heavy particles, in this work protons, is achieved, the possibility to fabricate detectors that can work under several extreme environments becomes plausible.

The main objective of this investigation consists in achieving a reproducible fabrication method to build GaN microwire based radiation sensors and analyse them in terms of their electrical and optical properties and their potential to detect UV light and proton radiation. Although the big majority of reports so far are relative to structures based on nanowires, we chose to use microwires instead because their larger volume makes them better suited for high energy particles and X-rays. In this way, the idea is to settle a compromise between the better crystalline quality associated to wire-based GaN and the larger volume of bulk GaN. On the other hand, the fact that microwires are larger, makes the fabrication process more straight forward.

II. EXPERIMENTAL METHODS

The GaN wires that were used for this investigation were grown by catalyst-free metal-organic chemical vapour deposition (MOCVD)[8]. MOCVD uses a combination of vapour phase precursors, in our case trimethyl gallium (TMGa) and ammonia (NH_3). These are ther-

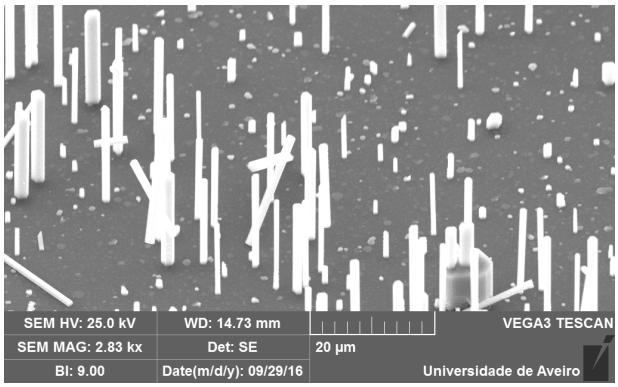

FIG. 1. SEM image obtained at an amplification of 2830× with a substrate tilt of 47°

mally decomposed at elevated temperatures to form the desired non-volatile product that is deposited on the substrate while the volatile product is carried away to the exhaust. The methodology is highly reproducible and can be based on three main steps: the initial substrate treatment, the GaN seed nucleation and the vertical growth. The microwires that were grown present diameters ranging from 1 μm to 2 μm and a length of approximately 20 μm. A silane flux of 45 sccm, used to improve the vertical growth of the wires during the first 13 μm, causes the incorporation of Si donors into the bottom part of the grown wires, leading to a highly doped section with a doping concentration in the $10^{19} - 10^{20}$ cm^{-3} range. Additionally, due to the silane a thin shell (< 3 nm) of SiN_x is formed around this part of the wire. In the upper part, since no silane flux was used, unintentionally doped n-type GaN, with a lower carrier concentration ($\sim 10^{18}$ cm^{-3}), is grown and no SiN_x sidewall layer exists. A full description of the growth process can be found in reference [8].

To verify the geometrical aspect of the microwires, scanning electron microscopy was done at the university of Aveiro. A typical image can be viewed in figure 1.

The vertically aligned microwires were detached from their growth template and transfered to a SiO2 coated Si wafer to allow the processing of planar structures. To successfully fabricate the radiation sensors, a methodology consisting of three main phases was followed. Firstly, with the knowledge that the placement of the microwires on the device substrate is random, a grid needs to be deposited. This grid will allow to define the position of the dispersed microwires using a system of coordinates. The structure of the grid consists of 150Å thick TiW deposited on top of a silicon substrate. To draw the desired pattern, photolithography was used and, finally, to avoid undesired contact between the wires and the TiW, an insulating layer of 2000 Å SiO_2 was deposited. The second stage is the deposition of the microwires. This was done by primarily detaching them from their Al_2O_3 growth substrate via ultrasound treatment. Afterwards, some droplets of the resulting suspension of microwires in isopropyl alcohol were deposited on the SiO_2. By optical microscopy and with the grid as reference, their position was defined. A metal lift-off process was used to deposit the contacts. First, a second photolithography was done to draw the desired pattern. Then 300Å of Cr and 4000Å of Au were deposited by magnetron sputtering. Finally, the lift-off was achieved by immersing the substrate into a microstrip solution which was then placed, subsequently, in a heat bath (60°C) and in a ultrasound bath (60°C) for 4 hours. To conclude, the subtrates were integrated on a chip carrier in order to allow *in-situ* measurements while performing proton irradiation. Figure 2 shows a microscopy image of a single sensor that was successfully fabricated.

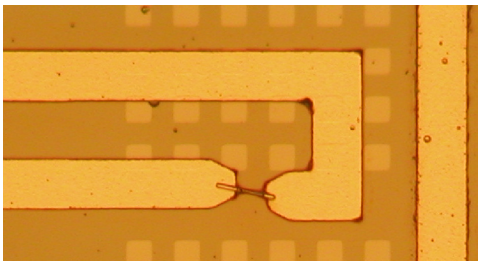

FIG. 2. Optical microscopy image of a microwire device after the lift-off step. The squares of the grid have a lateral size of 10 μm and the width of the contact paths is 20 μm

To characterize the fabricated devices, electrical and opto-electrical characterization was done. A two-probe configuration, connected to the Agilent B1500A Semiconductor Device Analyser, was used to make the measurements. This setup allows us to perform Current-voltage (I-V) characterization, which have been a popular characterization method for many years and are perhaps the easiest and most routine measurements performed. Nonetheless, they can provide valuable information about the intrinsic properties of the wires and about the quality of the contacts between the GaN and the metal[9].

For the photoconductivity measurements a 9 Watt Tungsten halogen lamp, a high brightness deuterium lamp and a high-power UV LED were used. When the devices are irradiated with light of one of these sources, electron-hole pairs are generated causing the subsequent increase in current - the photocurrent. Regarding the analysis of the excitation energy dependence, gain and decay time of the photocurrent, photoconductivity spectroscopy, steady-state I-V and transient I-V measurements were done.

The proton irradiation was done at the nuclear microprobe facilities at CTN (Campus Tecnológico Nuclear). The characteristic energy of the proton beam used in the experiments is 2 MeV and, in most cases, the beam current was set between 1 nA and 300 pA, while the irradiated area ranged from 25×25 μm^2 to 15×15 μm^2. This corresponds to a flux of $\sim 1 \times 10^{15}$ protons/cm^{2}s. The main goals of the measurements are to analyse, as

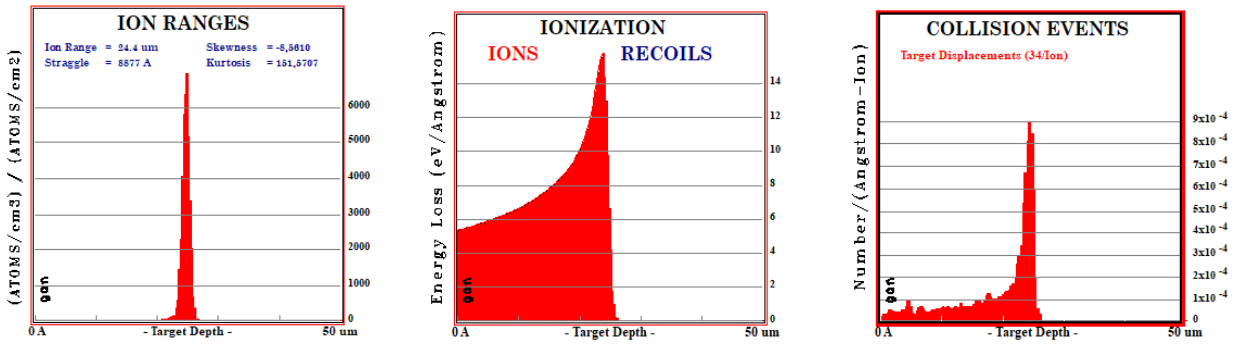

FIG. 3. The obtained results for a SRIM simulation with 2 MeV H^+ protons hitting a planar GaN target of thickness equal to 50 μm; The left graph plots the concentration of hydrogen atoms versus the target depth; The middle graph shows the energy loss due to ionization versus the target depth; The right graph the profile of displaced atoms.

mentioned, how the wires react to the high energy radiation in terms of current but as well to see how the wires are affected in terms of damage and defect creation. The results of a SRIM (stopping and ranges of ions in matter) simulation[10], shown in figure3, indicate that for an energy of 2 MeV, the protons easily go through the microwires and we can safely assume that no hydrogen implantation occurs. Furthermore, the ionization calculations indicate that for the first two 2 μm it can be considered constant. This allows us to conclude that, when we irradiate our wires with protons, the ionization profile will be constant across the entire microwire cross-section. Finally, the plot relative to the collision events, shows that there will be some damage creation, but since the protons cross the wires, the number of created defects will not be large.

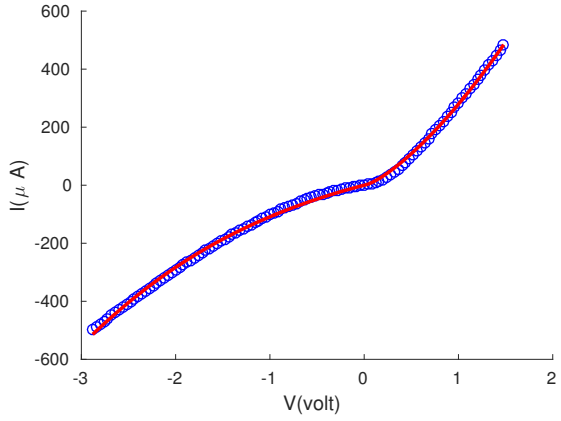

FIG. 4. Asymmetric I-V curve obtained for sample 216U. The red line corresponds to the experimental data and the blue circles correspond to the fit results.

III. RESULTS AND DISCUSSION

A. Electrical characterization

The electrical characterization showed that not all the devices presented the same I-V behaviour. Simply put, we can divide the results into four types of curves: almost linear, almost symmetric, asymmetric, and rectifying. After rapid thermal annealing (RTA) for 60 seconds at 400°, the overall response of the devices became more homogeneous and the most commonly obtained curves were asymmetric (fig.4). The asymmetry in the I-V curves can be attributed to the gradient of charge carriers along the microwire. As is well known, the thickness of the depletion width is proportional to the inverse square root of N_d[11]. Thus, for a higher N_d the tunnelling of electrons through the barrier becomes more significant, yielding a higher current. Consequently, for the highly doped end a more ohmic like contact is expected while for the top of the wire, the type of contact depends on whether the doping concentration is or not under the semiconductor metal transition.

By looking at the overall response of the devices there are two additional statements we can make. Firstly, the devices present high dark conductivity and, secondly, the obtained I-V curves show that the contacts are not exactly equivalent due to different contact areas and/or different interface properties. Regarding the former statement, most devices reach currents of 2 mA for a bias well below 5 Volts. This can be attributed to the high donor concentration in the microwires as a result of the growth process. Consequently the GaN becomes degenerate[8]. Microwires grown by an identical process as the ones used in this investigation were also studied by Tchoulfian *et al.*[12] and they also reported a very high conductivity. Their devices showed linear I-V curves however.

As we have non linear contacts, we can assume a back-to-back Schottky configuration and since doping is significant, we suspect that the electron transport is done through a mix of field emission and thermionic field emis-

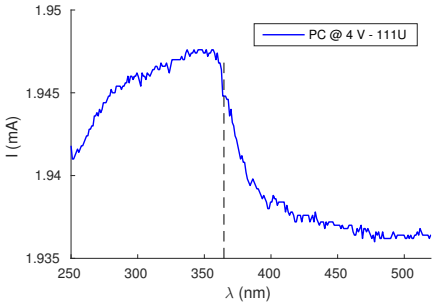

FIG. 5. The photoconductivity spectrum obtained with a 4V bias for the 111U device. The red dotted line represents the fit of the linear region in the absorption and the black dotted line represents the reported bandgap of 3.4 eV The spectrum has not been corrected.

sion. With this knowledge, we decided to analyse the obtained data with a program developed by Liu *et al.*[13]. Although the model fits our data adequately and the results for the barrier heights are in agreement with the symmetric, asymmetric and rectifying curves, the model fails to properly distinguish between the different sections of the devices and reveals ambiguities when comparing I-V curves under different radiation environments. Therefore, instead of applying the model to the entire bias range of the I-V curves, only the current at high voltages was considered. In this range, the voltage drop in the microwire exceeds the voltage drop at the Schottky barriers, which allows us to write $V \simeq V_{mw} = R_{mw}I$, from which the microwire resistance can be extracted.

B. Photoconductivty

To study the photoconductive properties of the devices spectroscopy, static I-V and transient I-V measurements upon irradiation with light were performed. Figure 5 represents the obtained photoconductivity spectrum (PCS) for sample 111U.

If we take a look at the general shape of the PCS and analyse it qualitatively, we can see that it follows the expected behaviour. The photocurrent is low for excitation below the bandgap and absorption increases for wavelengths close to the bandgap. The physical explanation for these occurrences are straight forward, since the bandgap of GaN is wide, incident radiation with energy well below E_g will not generate any excess carriers as the electrons do not receive sufficient energy to make the transition from the valence to the conduction band. When the energy of the radiation increases to values closer to E_g, the higher energy states in the conduction band become available and electrons start to occupy them, creating an excess of electrons and, consequently, the current increases. Although these observations are obvious, they give strong evidence that, generally speaking, the devices work as expected regarding their absorption capacities.

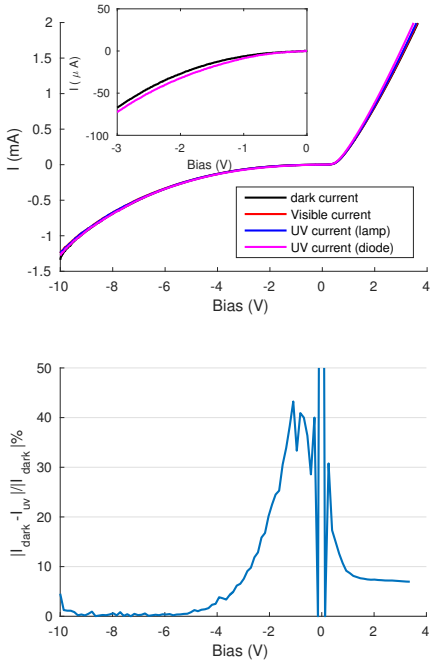

FIG. 6. IV characteristics the 210U device under dark (black curve) conditions, when irradiated with visible light (red curve) and when irradiated with two different UV sources, the Deuterium lamp(magenta curve) the high-power and UV led (purple curve) (top); On the right hand side the respective gain factor between the dark current and the photocurrent obtained with the high power LED is plotted (bottom).

The visible sub bandgap tail can be associated to the typical Urbach edge which can be caused by perturbations due to defects[14]. When these defect levels contain trapped holes or electrons and are excited by photons, excess carriers can be generated. Since the levels are localized somewhere in between the valence and conduction band, the energy of excitation is lower than E_g[15]. In the present case it is likely that surface defects created during device processing play a role in this sub-gap absorption.

In figure6 the I-V characteristics of photocurrents obtained with different light sources are compared with the dark current. As can be seen, the increase in current due to photoexcitation is small. This is more evident in the gain profile for the case of excitation with a UV diode, calculated by equation1 and also depicted in figure 6.

$$\Delta_I = \frac{I_{uv} - I_{dark}}{I_{dark}} \ . \tag{1}$$

The fact that our devices present a relatively low gain factor is not surprising since low photocurrent gain for heavily doped GaN nanowires was already observed previously.[16–18]. A possible explanation for this is that heavy doping limits the depletion width in dark environment to already very small values. Consequently, irradi-

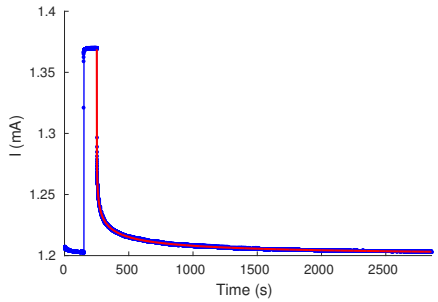

FIG. 7. Transient IV curve measured with device 229U; the light was turned on and off only once to calculate the decay time; The blue line corresponds to the experimental data and the red line corresponds to the fit result.

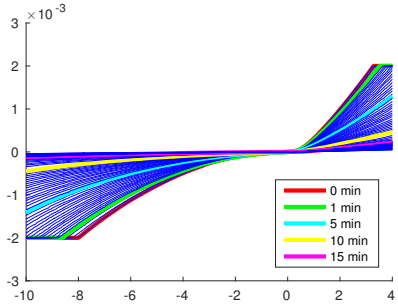

FIG. 9. The decay conductivity of the 110U device while being exposed to ionizing irradiation. The I-V curves over the full bias are shown where the legend indicates how long the device is exposed to the irradiation

ation with UV light will not drastically improve the electron transport through the wire as it does, for example, in fully depleted wires[16]. The origin of the photocurrent can therefore be attributed mostly to the generation of excess electrons by UV excitation, which only represents a small fraction of the electron concentration in the dark[18].

To study the decay time of the photocurrent after excitation transient I-V experiments, with the high power UV LED as light source, were performed. After turning the light on, we wait until the photocurrent reaches a stable value and then turned the light off again. To obtain the decay time with precision, we waited approximately 30 minutes before ending the measurement. To extract the decay time, the data was fitted using the following equation[19]

$$I = (I_{uv} - I_{dark}) \exp\left[-\left(\frac{t}{\tau_d}\right)^{\beta}\right] + I_{dark}, \qquad (2)$$

where the decay time is given by τ_d and β represents the exponential stretching parameter. The results for the 229U device are shown in figure7.

The obtained decay time for the presented curve is 3.97 ± 0.02 s while the exponential stretching parameter yielded 0.2117 ± 0.0002 s. The values obtained for other devices and different applied bias are of the same order. The values obtained for β are in agreement with some of the previous reported results for both GaN thin films and nanowires[20, 21]. Regarding τ_d, for a typical photodetector, a decay time of the order of a second is quite large. The long times are a consequence of the effects of persistent photocurrent (PPC), which has been widely reported in GaN thin film and nanowire devices. Nonetheless, when compared with reported values for GaN nanowires ($\tau_d > 100$s) and thin films ($\tau_d > 1000$s) our decay times are relatively fast[5, 22]. This might be due to the superior crystalline quality of microwires when compared to thin films and reduced influence of the surface when compared to nanowires.

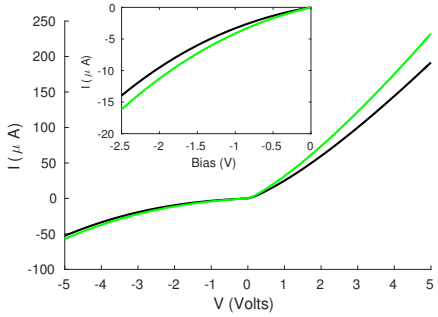

FIG. 8. The obtained I-V curve when performing electrical measurements during proton irradiation and comparison with the I-V curve obtained under dark conditions.

C. Proton irradiation

The following step in the study of the sensors consists in exposing them to proton irradiation to test their radiation resistance and applicability as particle detectors. After the beam was aligned, the first experiments

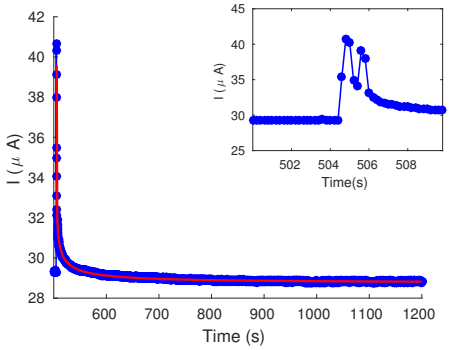

FIG. 10. I-t curve with an applied bias of 3V representing the response to ionizing radiation after a short pulse for the 229U device (the pulse is represented in more detail in the inset). The blue line corresponds to the experimental data and the red line corresponds to the fit result.

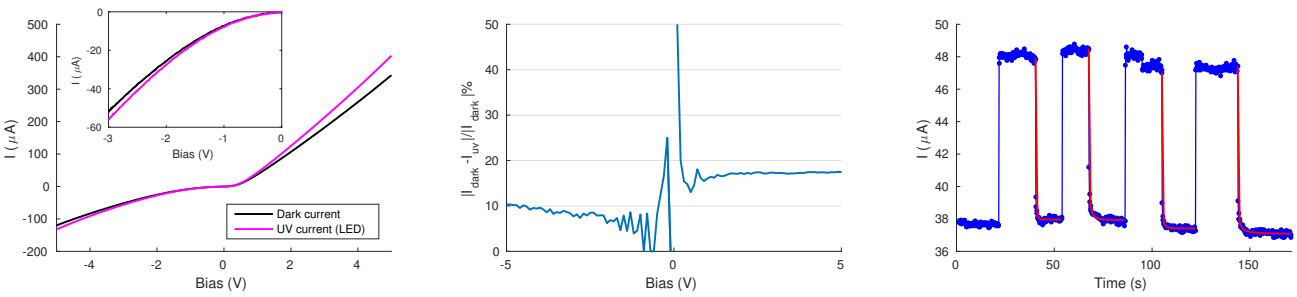

FIG. 11. In the left graph I-V curves for the 216U device are shown, the black curve corresponds to I_{dark} and the magenta curve to I_{uv} and in the middle graph the respective gain ratio is plotted; The right graph contains transient I-V measurements at -3 volts for the 216U device. Since the decay time for negative bias is fast, the UV light was turned on and off several times. The blue dots correspond to the experimental data and the red lines to the respective fits.

consisted in measuring the change in current due to the ionizing irradiation. To obtain a full I-V curve under exposure to protons, the beam area was set to 20×20 μm^2 and the current to 300 pA, which corresponds to a flux of 5×10^{14} protons/cm^{2}s. In figure 8 the obtained I-V curve is compared with an I-V curve measured under dark conditions immediately before irradiation. The main difference between the obtained results with proton radiation when compared to the results obtained with UV radiation are the higher gain values obtained in the former. This can be attributed, on one hand, to the higher excitation density and, on the other hand, to the higher excitation depth. Since the energies involved are much higher, each proton will generate more excess carriers than a photon during UV irradiation, hence the larger density. Regarding the depth, as was extracted from the SRIM simulations, the protons cross the entire wire and excitation occurs both at the surface and in the bulk region whereas the UV radiation causes mostly excitations at the surface and it is not likely that it penetrates much deeper into the wire.

To verify the effects of the irradiation on the overall performance of the devices, these were continuously exposed to protons for a longer time interval. At the same time, their I-V characteristics were being measured. The resistance of a large quantity of curves was extracted by fitting the data and the resistance increased from approximately 1.9 kΩ before exposure to irradiation, to almost 200 kΩ after 30 minutes of exposure to irradiation (corresponding to a flux of 5×10^{14} protons/cm^{2}s). The decay in conductivity as a consequence of irradiation makes it harder to perform stable transient I-V measurements. However, since the response time of our devices is relatively fast, this could be overcome by only turning the beam on for a single instant, short enough to avoid significant defect creation and long enough to reach the saturation current. The obtained curve is depicted in figure 10 and the resulting decay time is $\tau_d = 0.628 \pm 0.009$. The values for other measurements of the same type yielded similar results. If we thus compare the decay times from the transient obtained with UV excitation, we can see that they are one order of magnitude smaller. One possible explanation is that the higher penetration depth of the protons make the recombination less dependent on the surface when compared to UV excitation.

D. Proton irradiation effects on photoconductivity

As observed, the ionizing radiation has severe consequences on the overall conductivity of the sensors. It is therefore fundamental to redo the optical measurements in order to see whether the response of the devices is maintained. To recover some of the defects created by the proton irradiation, firstly a RTA step at 600°C for 120 seconds was done. Then, the same I-V measurements as prior to the irradiation were done. The obtained results are shown in figure 11

If we compare the responsivity of the devices to the UV light before and after the irradiation, we can see that it has been improved for the latter case. Prior to the irradiation, the gain factor at negative bias was negligible whereas after irradiation the gain factor reaches 10% at a bias of -5 volt. For a positive bias, the gain also increased significantly, from around 10% to nearly 20%. Another interesting fact is that the gain at negative bias is not constant, but rather increases if we apply a larger bias. Interesting to see is that the shape of the gain plots is very similar to the ones obtained before irradiation. This is a good indication that the mechanisms behind the photocurrent generation are the same and that only the magnitude of the dark current decreased. The comparatively larger increase in the photocurrent gain can be explained following the carrier removal due to the irradiation. As the amount of carriers in the dark case is now smaller, the amount of excess carriers generated when the excitation occurs, represent a bigger fraction, hence the increased gain factor.

Additionally, the decay time at negative bias is surprisingly fast, up to two orders of magnitude below the decay times at positive bias. Unfortunately, no measurements at $V < 0$ V could be done before the irradiation

due to the low response, so we can not directly say that the fast decay times are a consequence of the irradiation. Nonetheless, the enhancement of the decay time after exposure to protons has been observed previously for thin films[23]. The partial removal of the deep acceptor states by the proton irradiation was suggested as a possible cause because a quenching of the yellow band, typically associated to transitions between deep acceptor states and the conduction band was observed as well while performing SPC measurements after the irradiation[23].

IV. CONCLUSIONS

The goal of this work was to develop radiation sensors based on GaN microwires, with special interest towards their capability to detect protons. The performed optoelectrical characterization measurements revealed that the bandgap of the GaN was well defined and no significant absorption in the visible spectrum was observed. The photocurrent gain of the fabricated photodectectors is however still too low to be interesting for application in actual devices. The main cause for this occurrence is the high doping concentration, as this leads to a very large dark current, despite the presence of Schottky barrier at the metal-semiconductor interface. Despite the low gain factors we obtained, transient measurements revealed faster decay times in comparison to most reports on GaN nanowire or thin film based photodetectors.

Our findings based on the proton-irradiation studies with the detectors revealed promising results. Higher current gain factors upon proton irradiation were obtained compared to the gain observed for UV irradiation and, after excitation, the time it took the devices to return to the stable dark current was smaller to those obtained after UV excitation. Thus, similar results were obtained for both UV and proton excitation, which indicates that GaN microwires have the potential to be applied in radiation detectors in the same way as they are already applied in UV photodetectors. Finally, the irradiated devices were annealed and tested again regarding their UV detection potential. The results indicated overall improved responses and the photocurrent gain increased to approximately twice the values obtained prior to the irradiation. Promising results regarding faster decay times for negative were also obtained.

ACKNOWLEDGMENTS

D. Verheij would like to thank Dr. Katharina Lorenz for all the good advice and shared knowledge and Dr. Marco Peres for his great support during the experimental procedures, Prof. Susana Freitas and the process engineers at INESC-MN for help with the fabrication process, Dr. L.C. Alves for help with the irradiation of the devices, J. Eymery for providing the microwire samples and Prof. Teresa Pinheiro and Dr. N.B. Sedrine for sharing the SEM images. Financial support by FCT Portugal (UID/FIS/50010/2013) for this investigation is gratefully acknowledged.

[1] I. Akasaki, "Fascinating journeys into blue light (nobel lecture)," *Annalen der Physik*, vol. 527, no. 5-6, pp. 311–326, 2015. [Online]. Available: http://dx.doi.org/10.1002/andp.201500803

[2] Q. Chen, J. W. Yang, A. Osinsky, S. GaNgopadhyay, B. Lim, M. Z. Anwar, M. A. Khan, D. Kuksenkov, and H. Temkin, "Schottky barrier detectors on GaN for visible–blind ultraviolet detection," *Applied Physics Letters*, vol. 70, no. 17, pp. 2277–2279, 1997. [Online]. Available: http://dx.doi.org/10.1063/1.118837

[3] C. M. Lieber and Z. L. Wang, "Functional nanowires," *MRS Bulletin*, vol. 32, no. 2, p. 99–108, 2007. [Online]. Available: http://dx.doi.org/10.1557/mrs2007.41

[4] L. Rigutti and M. Tchernycheva, *GaN Nanowire-based Ultraviolet Photodetectors*. John Wiley & Sons, 2014, pp. 179–202.

[5] R. Calarco, M. Marso, T. Richter, A. I. Aykanat, R. Meijers, A. v.d. Hart, T. Stoica, and H. Lüth, "Size-dependent photoconductivity in MBE-grown GaN-nanowires," *Nano Letters*, vol. 5, no. 5, pp. 981–984, 2005, pMID: 15884906. [Online]. Available: http://dx.doi.org/10.1021/nl0500306

[6] E. Schlenker, A. Bakin, T. Weimann, P. Hinze, D. H. Weber, A. Gölzhäuser, H.-H. Wehmann, and A. Waag, "On the difficulties in characterizing ZnO nanowires," *Nanotechnology*, vol. 19, no. 36, p. 365707, 2008. [Online]. Available: https://doi.org/10.1088/0957-4484/19/36/365707

[7] H.-Y. Chen, R.-S. Chen, N. K. Rajan, F.-C. Chang, L.-C. Chen, K.-H. Chen, Y.-J. Yang, and M. A. Reed, "Size-dependent persistent photocurrent and surface band bending in *m*-axial GaN nanowires," *Phys. Rev. B*, vol. 84, p. 205443, Nov 2011. [Online]. Available: http://dx.doi.org/10.1103/PhysRevB.84.205443

[8] R. Koester, J. S. Hwang, C. Durand, D. L. S. Dang, and J. Eymery, "Self-assembled growth of catalyst-free GaN wires by metal–organic vapour phase epitaxy," *Nanotechnology*, vol. 21, no. 1, p. 015602, 2010. [Online]. Available: http://dx.doi.org/10.1088/0957-4484/21/1/015602

[9] M. Brinza, J. Willekens, M. Benkhedir, and G. Adriaenssens, *Photoconductivity in Materials Research*. Boston, MA: Springer US, 2007, pp. 137–146. [Online]. Available: https://doi.org/10.1007/978-0-387-29185-7_7

[10] J. F. Ziegler, J. P. Biersack, and U. Littmark, Eds., *The Stopping and Range of Ion in Solids*. New York: Pergamon, 1985.

[11] D. A. Neaman, Ed., *Semiconductor Physics and Devices*, 3rd ed. New York: McGraw-Hill, 2003.

[12] P. Tchoulfian, F. Donatini, F. Levy, B. Amstatt, P. Ferret, and J. Pernot, "High conductivity in Si-doped GaN wires," *Applied Physics Letters*, vol. 102, no. 12, p. 122116, 2013. [Online]. Available: http://dx.doi.org/10.1063/1.4799167

[13] Y. Liu, Z. Y. Zhang, Y. F. Hu, C. H. Jin, and L.-M. Peng, "Quantitative fitting of nonlinear Current-Voltage curves and parameter retrieval of semiconducting nanowire, nanotube and nanoribbon devices," *Journal of Nanoscience and Nanotechnology*, vol. 8, no. 1, pp. 252–258, 2008. [Online]. Available: http://doi.org/10.1166/jnn.2008.N04

[14] D. Redfield and M. A. Afromowitz, "The direct absorption edge in covalent solids," *Applied Physics Letters*, vol. 11, no. 4, pp. 138–140, 1967. [Online]. Available: http://dx.doi.org/10.1063/1.1755067

[15] M. Salis, A. Anedda, F. Quarati, A. J. Blue, and W. Cunningham, "Photocurrent in epitaxial GaN," *Journal of Applied Physics*, vol. 97, no. 3, p. 033709, 2005. [Online]. Available: http://dx.doi.org/10.1063/1.1848191

[16] F. González-Posada, R. Songmuang, M. Den Hertog, and E. Monroy, "Room-temperature photodetection dynamics of single GaN nanowires," *Nano Letters*, vol. 12, no. 1, pp. 172–176, 2012, pMID: 22142411. [Online]. Available: http://dx.doi.org/10.1021/nl2032684

[17] T. Richter, H. L. R. Meijers, R. Calarco, and M. Marso, "Doping concentration of GaN nanowires determined by opto-electrical measurements," *Nano Letters*, vol. 8, no. 9, pp. 3056–3059, 2008, pMID: 18687013. [Online]. Available: http://dx.doi.org/10.1021/nl8014395

[18] L. Rigutti, M. Tchernycheva, A. De Luna Bugallo, G. Jacopin, F. H. Julien, L. F. Zagonel, K. March, O. Stephan, M. Kociak, and R. Songmuang, "Ultraviolet photodetector based on GaN/AlN quantum disks in a single nanowire," *Nano Letters*, vol. 10, no. 8, pp. 2939–2943, 2010, pMID: 20617803. [Online]. Available: http://dx.doi.org/10.1021/nl1010977

[19] C. H. Qiu and J. I. Pankove, "Deep levels and persistent photoconductivity in GaN thin films," *Applied Physics Letters*, vol. 70, no. 15, pp. 1983–1985, 1997. [Online]. Available: http://dx.doi.org/10.1063/1.118799

[20] J. Z. Li, J. Y. Lin, H. X. Jiang, A. Salvador, A. Botchkarev, and H. Morkoc, "Nature of Mg impurities in GaN," *Applied Physics Letters*, vol. 69, no. 10, pp. 1474–1476, 1996. [Online]. Available: http://dx.doi.org/10.1063/1.116912

[21] H. M. Chen, Y. F. Chen, M. C. Lee, and M. S. Feng, "Persistent photoconductivity in n-type GaN," *Journal of Applied Physics*, vol. 82, no. 2, pp. 899–901, 1997. [Online]. Available: http://dx.doi.org/10.1063/1.365859

[22] A. Winnerl, R. N. Pereira, and M. Stutzmann, "Kinetics of optically excited charge carriers at the GaN surface," *Phys. Rev. B*, vol. 91, p. 075316, Feb 2015. [Online]. Available: https://doi.org/10.1103/PhysRevB.91.075316

[23] A. Castaldini, A. Cavallini, and L. Polenta, "Radiation-induced effects in GaN by photoconductivity analysis," *physica status solidi (a)*, vol. 202, no. 15, pp. 2912–2919, 2005. [Online]. Available: http://dx.doi.org/10.1002/pssa.200521110